# Invadolysin, a conserved lipid-droplet-associated metalloproteinase, is required for mitochondrial function in *Drosophila*

**Francesca Di Cara[1,*], Edward Duca[1,‡], Donald R. Dunbar[1], Gerard Cagney[2] and Margarete M. S. Heck[1,§]**

[1]University of Edinburgh, Queen's Medical Research Institute, BHF/University Center for Cardiovascular Science, 47 Little France Crescent, Edinburgh EH16 4TJ, UK
[2]Conway Institute, University College Dublin, Belfield, Dublin 4, Ireland

*Present address: Department of Biological Sciences, University of Alberta: G-502 Biological Sciences Building, Edmonton, Alberta T6G 2E9, Canada
‡Present address: University of Malta, Msida, MSD 2080, Malta
§Author for correspondence (margarete.heck@ed.ac.uk)

*Accepted 26 July 2013*
*Journal of Cell Science 126, 4769–4781*

*doi: 10.1242/jcs.133306*

## Summary

Mitochondria are the main producers of ATP, the principal energy source of the cell, and reactive oxygen species (ROS), important signaling molecules. Mitochondrial morphogenesis and function depend on a hierarchical network of mechanisms in which proteases appear to be center stage. The *invadolysin* gene encodes an essential conserved metalloproteinase of the M8 family that is necessary for mitosis and cell migration during *Drosophila* development. We previously demonstrated that invadolysin is found associated with lipid droplets in cells. Here, we present data demonstrating that invadolysin interacts physically with three mitochondrial ATP synthase subunits. Our studies have focused on the genetic phenotypes of *invadolysin* and *bellwether*, the *Drosophila* homolog of ATP synthase α, mutants. The *invadolysin* mutation presents defects in mitochondrial physiology similar to those observed in *bellwether* mutants. The *invadolysin* and *bellwether* mutants have parallel phenotypes that affect lipid storage and mitochondrial electron transport chain activity, which result in a reduction in ATP production and an accumulation of ROS. As a consequence, *invadolysin* mutant larvae show lower energetic status and higher oxidative stress. Our data demonstrate an essential role for *invadolysin* in mitochondrial function that is crucial for normal development and survival.

**Key words:** Invadolysin, ATP synthase, Mitochondria, Energy homeostasis, *Drosophila*

## Introduction

Mitochondria are ubiquitous organelles that regulate crucial processes essential for controlling energy balance, cell signaling, development, growth, production of damaging oxygen radicals, and apoptosis in the organism (Ackerman and Tzagoloff, 2005; Devenish et al., 2008; McBride et al., 2006; Newmeyer and Ferguson-Miller, 2003). Numerous studies have shown that mitochondria also control the metabolic status of the cell and cell cycle checkpoints (Ackerman and Tzagoloff, 2005; Mandal et al., 2005; Owusu-Ansah et al., 2008). Mitochondrial functions are critically dependent on both nuclear and mitochondrial gene expression. Most of the nuclear-encoded gene products are imported from the cytosol into mitochondria using at least four different strategies, including a classical presequence pathway, but also through a redox-regulated import mechanism, the formation of supercomplexes with the respiratory chain, and two-membrane coupling of translocases (Chacinska et al., 2009).

The major function attributed to mitochondria is a bioenergetic role in the production of ATP, which combines oxidative phosphorylation reactions taking place in the mitochondrial matrix to the reductive processes of the mitochondrial electron transport chain (ETC) occurring in the inner membrane of the mitochondria (Devenish et al., 2008). Enzymes of the mitochondrial ETC are conserved throughout evolution (Talamillo et al., 1998; Viñas et al., 1990). The mitochondrial respiratory chain comprises one proton-translocating and four electron-transporting complexes, which produce ATP and accumulate reactive oxygen species (ROS) at various points. The metabolism of carbohydrates and proteins generates metabolic intermediates that feed electrons into the respiratory chain; electrons are passed from complex I to complex IV. This energy is used to pump protons out of the mitochondrial matrix, generating a membrane potential that is used by ATP synthase to synthesize ATP. ATP synthase is a multi-subunit complex found in the mitochondrial inner membrane in eukaryotes and in the inner membrane of bacteria (Talamillo et al., 1998). It is composed of two large structural moieties, $F_o$ and $F_1$. $F_o$ is the proton pump, whereas $F_1$ enzymatically generates ATP from ADP and inorganic phosphate. In eukaryotes, ATP synthase is formed from at least 15 different subunits that vary in their stoichiometry depending on the species (Wilkens, 2000). ATP synthase is commonly referred to as complex V of the respiratory chain.

Defects in mitochondrial respiratory chain enzymes affect mitochondrial membrane potential and result in the accumulation of ROS and defects in ATP synthesis. These changes affect cellular energy levels and cause oxidative stress, which have dramatic and deleterious impacts on development. Mutations that

affect the function of respiratory chain enzymes have been reported to affect energy levels and oxidative stress in flies, rats and humans (Bell et al., 2007; Celotto et al., 2006; Mourikis et al., 2006; Saleh et al., 2008).

We have previously described the identification and characterization of *invadolysin*, a novel essential gene encoding the sole member of the M8 class of metzincin metalloproteinases (McHugh et al., 2004). The gene was first identified in *Drosophila* based on intriguing mutant phenotypes, which included defects in mitotic progression and in germ cell migration. Larvae homozygous for *invadolysin* mutant alleles presented pleiotropic phenotypes including defects in chromosome structure, spindle formation, nuclear envelope dynamics, germ cell migration and lipid storage (Cobbe et al., 2009; McHugh et al., 2004). We have shown by immunolocalization and subcellular fractionation that invadolysin is localized to the surface of lipid droplets (Cobbe et al., 2009). The protein, which is conserved among metazoa, is homologous to Leishmanolysin or GP63 – a major surface protease that is postulated to facilitate dissemination of the *Leishmania* parasite.

In this study, we utilized biochemical, genetic and behavioral analyses to identify and characterize proteins that interact with invadolysin in *Drosophila*. We show that invadolysin interacts physically with ATP synthase subunits α, β and d. ATP synthase α (*bellwether*) and *invadolysin* mutants have many aspects of phenotype in common. Loss of *invadolysin* compromises the electron transport chain of the mitochondrial internal membrane resulting in decreased ATP and increased ROS production. These alterations trigger a signaling cascade that affects cell growth, the cell cycle, fatty acid synthesis and the stress response. Our discovery contributes both to the understanding of the action of invadolysin and the control of mitochondrial physiology.

## Results

Previous characterization of the *invadolysin* mutant phenotype in *Drosophila* showed that the gene was essential for viability, with mutant animals exhibiting defects in mitotic progression, cell migration and lipid storage (McHugh et al., 2004). Homozygous mutant animals died at the third-instar larval stage (McHugh et al., 2004). To better understand the role of invadolysin in development, we identified cellular components that invadolysin interacted with. To this end, we generated transgenic flies carrying a *pUAST-HA-invadolysin* construct (Fig. 1A) (Spradling and Rubin, 1982). Crucially, we demonstrated that HA–invadolysin could rescue *invadolysin* lethality when ectopically expressed in the spatiotemporal profile of the *armadillo* gene (data not shown). Restricted expression was required because ectopic ubiquitous expression of HA–invadolysin in a wild-type genetic background resulted in lethality. In order to use HA–invadolysin as a tool to identify biochemical interactors of invadolysin, we restricted expression of HA–invadolysin to a single non-essential tissue – using Gal4 driven by Glass Multiple Reporter (GMR-Gal4) (Li et al., 2012) to express HA–invadolysin in adult eyes (Brand and Perrimon, 1993; Moses and Rubin, 1991) (Fig. 1B). HA–invadolysin and interacting proteins were immunoprecipitated from lysates of fly heads using a commercial anti-HA affinity matrix. Lysate from non-transgenic wild-type adult heads served as the control. Seven protein bands were consistently observed when HA–invadolysin-precipitated samples were stained with colloidal Coomassie Blue (Fig. 1C). The samples were identified using Multidimensional Protein Identification Technology (MudPIT)-enabled mass

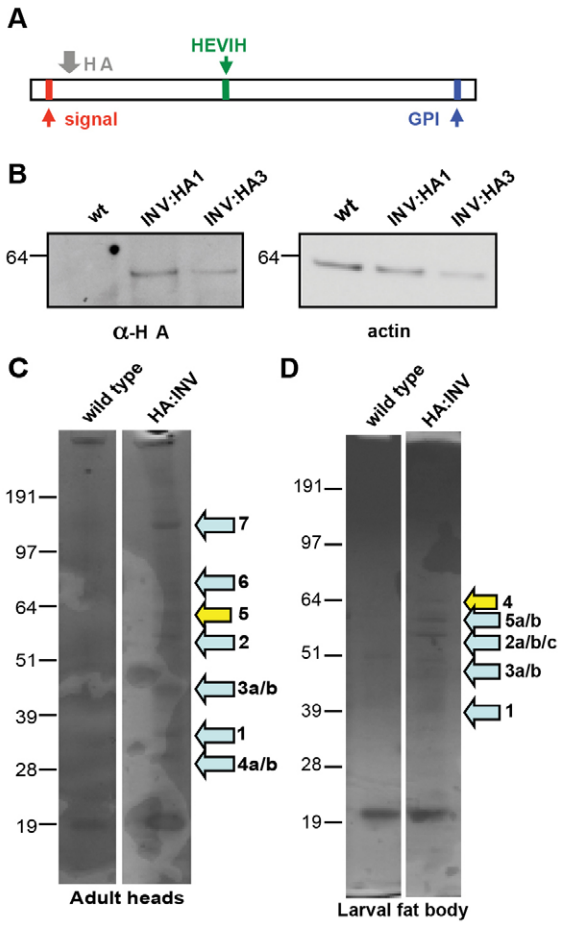


**Fig. 1. Invadolysin interacts with mitochondrial Complex V subunits.** (A) Diagram illustrating the HA–invadolysin construct that is integrated into the transgenic flies used in this study. The red, green and blue boxes indicate the predicted signal sequence, metalloproteinase motif, and the GPI-addition sites in the invadolysin sequence, respectively. The gray arrow denotes the insertion site of the HA tag. (B) HA–invadolysin was successfully expressed in fly heads of different transgenic lines using the GMR-Gal4 driver. A band of 62 kDa was detected in transgenic fly head extracts probed with an anti-HA antibody. This band was not detected in wild-type (wt) head extracts. (C) HA–invadolysin was immunoprecipitated from *Drosophila* head extracts (control and transgenic) and (D) larval fat body using a commercial anti-HA affinity matrix. All proteins that bound in the control extract were subtracted from the HA–invadolysin data set. In panels C and D, yellow arrows indicate the band that corresponds to invadolysin. Numbered arrow indicate the following proteins: 1, 3a and 3b, ATP syn-d, ATP syn-β and ATP syn-α (*bellwether*) subunits of the mitochondrial ATP synthase complex, respectively; 2 and 2a, heat shock protein cognate 3; 4a and 4b, tropomyosin 1 and tropomyosin 2, respectively; 6, heat shock protein 83; 7, myosin heavy chain; 2b, histone H3; 2c, heat shock protein cognate; 5a, larval serum protein 1γ; 5b, β-tubulin.

spectrometry (Yates et al., 1995). All peptides that were associated with the wild-type control beads (e.g. the band at 20 kDa) were removed from the HA–invadolysin data set.

Mass spectrometry analysis identified six significant hits in the HA–invadolysin sample. Surprisingly, three subunits of the mitochondrial ATP synthase complex (α, β and d) were present, represented by numerous peptides in two separate bands and reproduced in three separate experiments (supplementary material Table S1, S4). To determine whether

this interaction was specific to the eye, we also expressed HA–invadolysin in larval fat body (utilizing cg-Gal4 as a driver). Five protein bands were consistently observed when HA–invadolysin was immunoprecipitated from fat body lysates (Fig. 1D). Strikingly, the same three subunits of the ATP synthase complex (α, β and d) were also identified in fat body, represented by numerous peptides in two separate bands (supplementary material Tables S2, S4). These results demonstrate an interaction of invadolysin with the ATP synthase complex in two different tissues, suggesting that invadolysin might play a general role in regulating mitochondrial function. Although we attempted to perform the reciprocal physical experiment by immunoprecipitating ATP synthase from fly tissue lysates (and probing for invadolysin), none of the commercially available antibodies recognizing ATP syn-α immunoprecipitated ATP synthase from fly-head lysates.

### Genetic interaction of *invadolysin* and *ATP syn-α* (*bellwether*)

In eukaryotes, ATP synthase contains at least 15 subunits encoded by both nuclear and mitochondrial genes (Pedersen et al., 2000; Wilkens, 2000; Xing et al., 2005), which are well conserved in *Drosophila*. The three subunits binding to HA–invadolysin (ATP syn-α, ATP syn-β and ATP syn-d) are all encoded by nuclear genes. ATP syn-α and syn-β are found in the $F_1$ moiety of the enzyme where they both play a central role in enzymatic activity, whereas ATP syn-d is part of the $F_o$ proton channel.

We have recently shown that invadolysin is localized to lipid droplets in various human and mouse cell lines, and that triglyceride levels are lower in *invadolysin* mutant fat body (Cobbe et al., 2009). Importantly, a number of recent proteomic screens have found ATP synthase subunits in association with lipid droplets: ATP syn-α and -β in *Drosophila* embryos (Cermelli et al., 2006), ATP syn-α, -β, -b and -d in third-instar larvae (Beller et al., 2006), ATP syn-α, -β and -δ subunits in human adipocytes (DeLany et al., 2005), and ATP syn-β in mouse adipocytes (Brasaemle et al., 2004; Dugail and Hajduch, 2007). Thus, independent evidence linking ATP synthase subunits to both mitochondria and lipid droplets exists.

Therefore, in order to establish whether the physical interaction between invadolysin and ATP synthase subunits was of functional significance, we turned to genetic and physiological approaches. To investigate the genetic interaction between *invadolysin* and ATP synthase, we utilized two mutant alleles of the *ATP syn-α* (*bellwether*) gene (Galloni, 2003; Talamillo et al., 1998) in an enhancer/suppressor genetic assay (St Johnston, 2002). Overexpression of *invadolysin* in adult eyes using the GMR-Gal4 driver at 29°C results in a rough eye phenotype (supplementary material Fig. S1; Fig. 2A). Scanning electron microscopy analysis of the ommatidia in these eyes demonstrated tissue degradation and empty bristle sockets (supplementary material Fig. S1, arrow). *GMR-Gal4>pUAST-inv* homozygous flies were crossed with *bellwether* flies. We hypothesized that if a genetic interaction existed between the two genes, an alteration of *bellwether* expression might modify the rough eye phenotype induced by invadolysin overexpression. Both the $blw^{KG05893}$ and $blw^{EY08188}$ mutant alleles enhanced the rough eye (Fig. 2). In contrast, the control CyO balancer chromosome in the *GMR-Gal4>pUAST-inv* genetic background did not modify the rough eye phenotype. As an additional control, we observed that the rough eye caused by *GMR-Gal4>pUAST-inv* was suppressed by the $inv^{4Y7}$ mutant allele

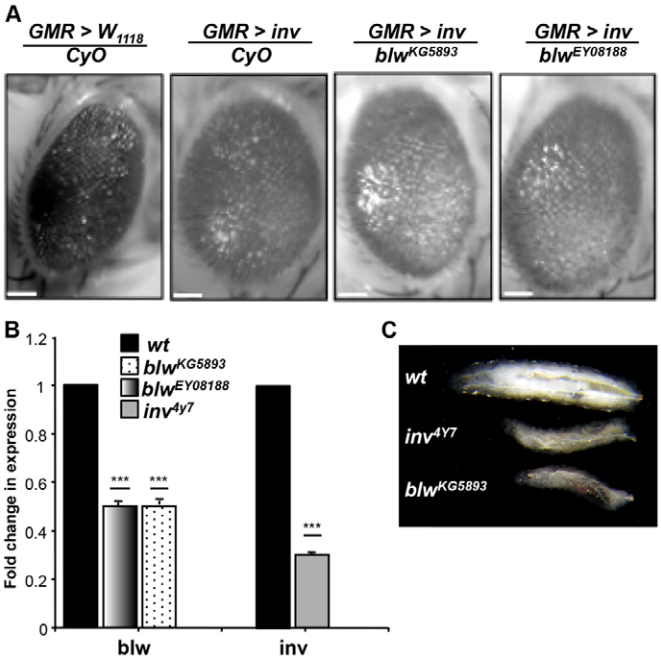


**Fig. 2. Genetic interaction between invadolysin and bellwether.** (A) Overexpression of *UAS-inv* in fly eyes under control of the *GMR-Gal4* driver results in a rough eye phenotype. Enhancement of the rough eye phenotype is observed with a copy of mutant *bellwether* ($blw^{KG05893}$ and $blw^{EY08188}$). Scale bars: 8 μm. (B) Transcriptional profile of bellwether and invadolysin transcripts in the respective homozygous mutant larvae. (C) $inv^{4Y7}$ and $blw^{KG05893}$ mutant larvae are much smaller than wild-type (wt) larvae at 5 days after hatching.

(data not shown). The observed genetic interaction between *invadolysin* and *bellwether* supports the hypothesis that the two proteins might act in the same or related pathways.

### *invadolysin* and *bellwether* mutant animals exhibit similar phenotypes

*invadolysin* mutant animals have growth and mitotic defects that result in smaller larvae lacking imaginal discs (McHugh et al., 2004). Recent studies have demonstrated that defects in other nuclear-encoded mitochondrial genes also affect cell growth and mitotic checkpoint control (Liao et al., 2006; Mandal et al., 2005; Owusu-Ansah et al., 2008), and one *bellwether* allele (not used in this study) was isolated in a screen aimed at identifying genes involved in growth signaling (Galloni and Edgar, 1999; Wilk et al., 2004). The *bellwether* homozygous animals show DNA replication and larval growth defects resulting in lethality during the larval instars, with no homozygous animals reaching the pupal stage (similar to the *invadolysin* mutant larvae). We showed that the $blw^{KG05893}$ allele (Bellen et al., 2004) interacted genetically with $inv^{4Y7}$. $blw^{KG05893}$ homozygous larvae were smaller than wild-type animals at the same stage, and the majority of animals died at the second-instar larval stage, with 20–30% of larvae reaching the third instar (Fig. 2C). Therefore both *bellwether* and *invadolysin* homozygous animals exhibit defects in larval development.

Mutations in genes encoding enzymes of the respiratory chain cause defects in mitochondrial ATP production. This in turn has an inhibitory effect on cellular anabolic pathways (Inoki et al.,

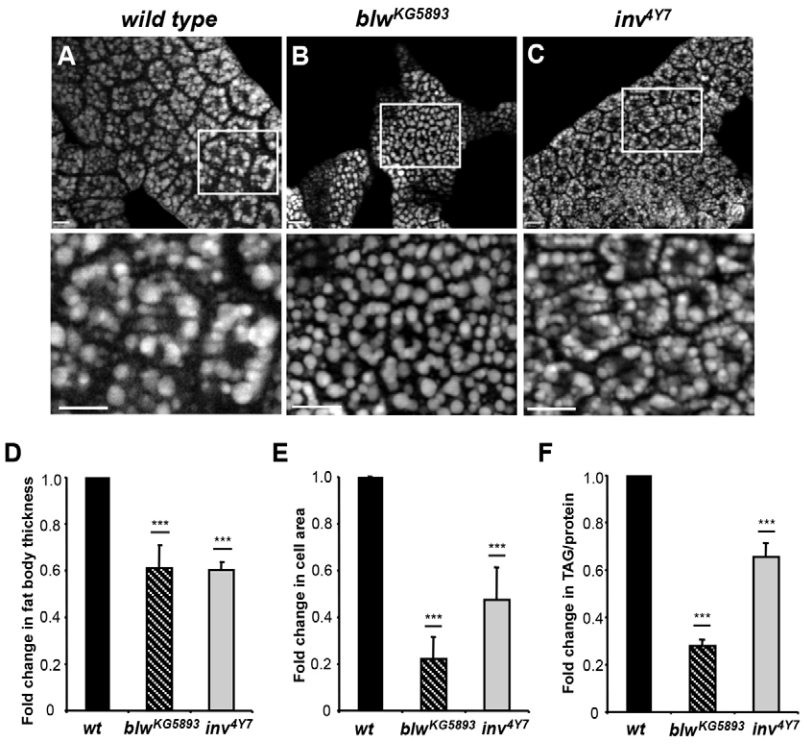


**Fig. 3. *bellwether* larvae exhibit reduced adipose tissue growth and triglyceride storage.** Visualization of lipid droplets within fat body cells from (A) wild-type, (B) $blw^{KG05893}$ and (C) $inv^{4Y7}$ larvae. As shown in the boxed areas enlarged below, $blw^{KG05893}$ and $inv^{4Y7}$ both affect larval fat body thickness and cell size compared to wild-type (wt) animals. Scale bars: 33 μm. (D) Mean thickness of fat body, with associated standard deviation ($n$=183). (E) Cross sectional area of cells, error bar shows standard deviation ($n$=41). (F) Quantification of total larval triglyceride normalized to total larval protein content. Error bars show associated standard deviation ($n$=3). ***$P$<0.001 compared with wild type, paired Student's $t$-test.

2003; Mourikis et al., 2006), thus accelerating catabolic pathways, such as lipid oxidation, to compensate for the drop in energy levels. We previously showed that $inv^{4Y7}$ affected both the thickness of the fat body and the size of fat body cells. We additionally found that the relative ratio of triglyceride to protein in $inv^{4Y7}$ larval extracts was significantly reduced (Cobbe et al., 2009). We therefore examined the fat body in homozygous third-instar $blw^{KG05893}$ larvae. When stained with the lipophilic dye Nile Red, fat body cell size appeared dramatically reduced compared to wild type (Fig. 3A–C). A dramatic reduction in the thickness of the fat body and the cross-sectional area of cells was observed in the homozygous $blw^{KG05893}$ larval fat body (Fig. 3D,E). We also observed that the ratio of triglyceride to protein content was significantly reduced in *bellwether* mutant larvae, as we demonstrated for *invadolysin* (Fig. 3F). Taken together, our observations reinforce the hypothesis that *invadolysin* and *bellwether*/*ATP syn-α* act in the same or parallel pathways.

### *invadolysin* and *bellwether* mutants regulate ETC activity

Although most subunits of the eukaryotic ATP synthase complex are encoded by nuclear genes, several other nuclear-encoded proteins are specifically involved in the biogenesis of ATP synthase (Ackerman and Tzagoloff, 2005). We hypothesize that the interaction between invadolysin and ATP synthase subunits might reflect a role in either assembly or function of the complex. In the absence of *invadolysin*, we predicted changes in mitochondrial morphology, number or activity.

To assess mitochondrial morphology and function in the $inv^{4Y7}$ and $blw^{KG05893}$ mutants, we stained the fat body of third-instar larvae with JC-1, a dye that labels all mitochondria independent of activity (Smiley et al., 1991), or MitoTracker, which labels only 'functional' mitochondria having a proton gradient. Third-instar

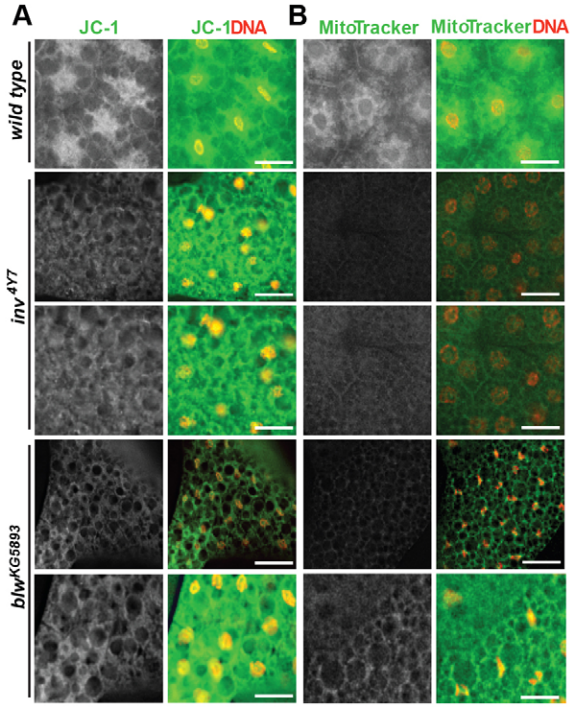


**Fig. 4. Mitochondrial activity is decreased in $inv^{4Y7}$ and $blw^{KG05893}$ larval fat body.** (A) Mitochondria are detectable in wild-type and mutant larval fat body cells, as visualized with the JC-1 mitochondrial marker (green), labeling all mitochondria independent of activity. DNA (red) is stained with DAPI. Scale bars: 20 μm. (B) Larval fat body cells labeled with MitoTracker (indicative of activity) are more intensely stained in wild-type third-instar larvae than in $inv^{4Y7}$ and $blw^{KG05893}$. DNA (red) is stained with DAPI.

JC-1-stained wild-type, $inv^{4Y7}$ and $blw^{KG05893}$ fat bodies showed that JC-1 readily accumulated in all of these tissues (Fig. 4A), suggesting that overall mitochondrial number was not grossly altered in $inv^{4Y7}$ and $blw^{KG05893}$ mutant cells. By contrast, staining with MitoTracker, showed decreased staining in $inv^{4Y7}$ and $blw^{KG05893}$ fat body in comparison to wild type, suggesting functional defects in both *invadolysin* and *bellwether* mitochondria (Fig. 4B). The appearance (diameter and length) of mitochondria in both $inv^{4Y7}$ and $blw^{KG05893}$ fat body cells following JC-1 staining was, however, altered when compared to wild type (Fig. 5A).

We used a second independent approach to assess the relative number of mitochondria in *invadolysin* and *bellwether* mutants because staining with either JC-1 or MitoTracker is inherently only qualitative. We determined the ratio of mitochondrial to nuclear DNA by measuring the ratio of the mitochondrial *cytochrome oxidase subunit I* (*CoI*) gene to the nuclear *actin 5C* gene in each genotype (Neretti et al., 2009). We observed that the ratio of *CoI* to *actin 5C* DNA was not changed in *invadolysin* and *bellwether* mutant larvae as compared to wild type (Fig. 5B). This observation suggested that the relative number of mitochondria was consistent, thus corroborating the results of the JC-1 staining, which showed little difference in labeling intensity between tissues (Fig. 4A).

**ATP levels are decreased in *invadolysin* third-instar larvae**

Studies in yeast, *Drosophila* and humans have shown that ATP syn-α is essential for the enzymatic activity of complex V in ATP production (Copeland et al., 2009; Lai-Zhang et al., 1999; Mráček et al., 2006). Mutations or drugs that inhibit ATP synthase activity reduce ATP production and should increase the cellular AMP:ATP ratio. We therefore measured ATP levels in *invadolysin* and wild-type larvae. The level of ATP in third-instar $inv^{4Y7}$ larvae was only 40% that of wild-type larvae (Fig. 5C). These data suggest that the accumulation of cellular ATP was severely affected upon mutation of *invadolysin*. Organisms have evolved compensatory mechanisms to mitigate the effects of energy reduction, and AMP activated kinase (AMPK) is a well-conserved kinase that functions as a sensor for cellular energy levels (Hardie, 2004). AMPK senses increased AMP levels under metabolic stress, and is activated by phosphorylation of Thr172 (Hardie, 2004). Activated AMPK downregulates anabolic pathways and upregulates catabolic pathways to maintain energy homeostasis in cells (Towler and Hardie, 2007). We therefore analyzed AMPK status in *invadolysin* mutant larvae compared to wild-type larvae. Although we observed no significant change in AMPK protein level in $inv^{4Y7}$ larval fat body, a significant increase in the phosphorylation of AMPK in $inv^{4Y7}$ extracts was apparent (Fig. 5D,D′). Therefore, loss of

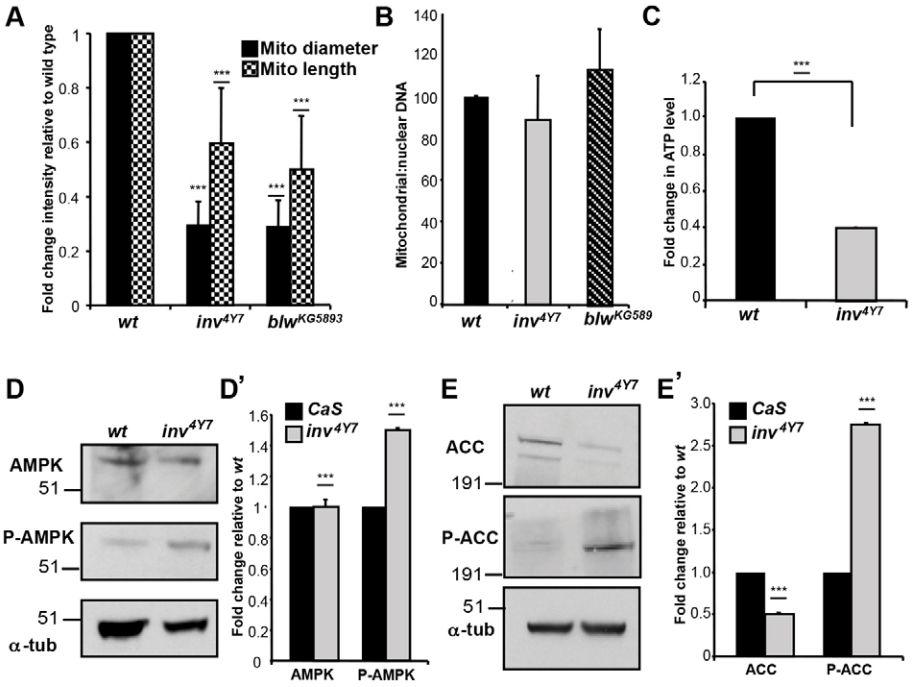


**Fig. 5. AMPK is activated in *invadolysin* mutants.** (A) Mean diameter and length of mitochondria in fat body cells following staining with JC-1, with standard deviations ($n$=388). ***$P$<0.001 compared with wild-type (wt), paired Student's $t$-test. (B) Mitochondrial DNA copy number is similar in $inv^{4Y7}$ to in control larvae. The mitochondrial DNA:nuclear DNA ratio was determined following qPCR for mitochondrial *CoI* (*cytochrome oxidase subunit I*) relative to nuclear *actin 5C*. Error bars show standard deviation. (C) $inv^{4Y7}$ third-instar larvae produce a lower amount of ATP than control larvae. Quantification of the total larval ATP level normalized to total larval protein content. Error bars show associated standard deviation. ***$P$<0.001, paired Student's $t$-test. (D,D′) Immunoblotting of third-instar larval fat body extract demonstrates that the level of AMPK is similar in control and $inv^{4Y7}$ samples. However, phospho-AMPK (P-AMPK) is increased in $inv^{4Y7}$ larvae. α-tubulin served as the loading control. (D′) Quantification of phosphorylated AMPK normalized to AMPK levels. Error bar represents the standard deviation derived from biological triplicate samples. ***$P$<0.001 compared with wild type (CaS), paired Student's $t$-test. (E,E′) Immunoblotting of third-instar larval fat body extract demonstrates that the level of ACC is decreased in *invadolysin* larvae, whereas the ACC phosphorylation (P-ACC) is increased in $inv^{4Y7}$ larvae. (E′) Quantification of phosphorylated ACC normalized to ACC levels. Error bar represents the standard deviation derived from biological triplicate samples. ***$P$<0.001 compared with wild-type (CaS), paired Student's $t$-test.

*invadolysin* affects mitochondrial function and reduces ATP production, resulting in activation of the energy sensor AMPK.

We then analyzed the role of AMPK in an *invadolysin* mutant background *in vivo* in an enhancer/suppressor genetic assay. The AMPK complex contains three subunits: the catalytic α subunit, the glycogen-sensing β subunit, and the γ subunit containing two regulatory sites that bind activating AMP and inhibitory ATP nucleotides. We crossed *GMR-Gal4>UAS-inv* flies with flies carrying a mutation in the *SNF4γ* gene (the γ subunit of *Drosophila* AMPK) (Lippai et al., 2008). The rough eye phenotype caused by overexpression of *invadolysin* was enhanced by a mutant copy of the *SNF4γ* gene (Fig. 6C). Our data suggest that *SNF4γ* usually responds to the level or activity of *invadolysin*, supporting our immunoblotting data showing AMPK activation in the *invadolysin* mutation.

In order to better understand the functional relationship between *invadolysin* and AMPK, we analyzed the viability of larvae fed the AMPK inhibitor Compound C or the AMPK activator AICAR (5-amino-4-imidazolecarboxamide ribonucleotide). When wild-type larvae were grown on Compound C, we observed no effect on their development (Fig. 6Ai,ii); 80% of $inv^{4Y7}$ mutant larvae, when grown on normal food, died after 5 days (prior to pupation), whereas 20% attempted pupariation. When fed Compound C, $inv^{4Y7}$ larvae lived for up to 7 days and attempted pupation (Fig. 6Aiii). Although the pupae were abnormal and unable to complete metamorphosis (as they lacked imaginal discs), this represented a greater longevity than on control food. Interestingly, wild-type larvae fed AICAR formed thinner pupae than usual and were unable to eclose, similar to $inv^{4Y7}$ pupae grown on Compound C (Fig. 6Aiv). *invadolysin* animals fed AICAR showed no discernable change in development (with larvae dying prior to pupation and only 10% attempting pupariation).

These *in vivo* experiments show that in the absence of *invadolysin*, AMPK was activated, which had the downstream consequence of developmental arrest of mutant animals. Importantly, this developmental arrest was partially overcome by *in vitro* feeding with Compound C, an AMPK inhibitor (Fig. 6A,B).

### ACC is inhibited in the *invadolysin* mutant

Once activated, AMPK switches on catabolic pathways to generate ATP, while switching off ATP-consuming processes such as biosynthesis, cell growth and proliferation; both are mediated by direct phosphorylation of substrates and indirectly, through effects on gene expression. One of the downstream effectors of AMPK in both flies and vertebrates is acetyl-CoA carboxylase (ACC, known as ACC1 or ACACA in vertebrates), which controls fatty acid synthesis in the mitochondrial matrix. ACC is inactivated by phosphorylation by AMPK (Ser93 in flies, Ser79 in mammals). Activation of AMPK in response to different stress conditions (reduced ATP levels, hypoxia or glucose deprivation) blocks lipid neo-synthesis, inactivating ACC (Ha et al., 1994). We hypothesized that mutation of *invadolysin* might affect ACC. Our results showed that the phosphorylation of ACC was indeed increased in $inv^{4Y7}$ fat body extract compared to wild type, whereas the overall level of ACC was lower in mutant animals (Fig. 5E,E′). Our data suggest that ACC was inactivated in *invadolysin* mutant animals, which should result in decreased fatty acid synthesis – consistent with our previous results that showed reduced triglyceride levels in $inv^{4Y7}$ larvae.

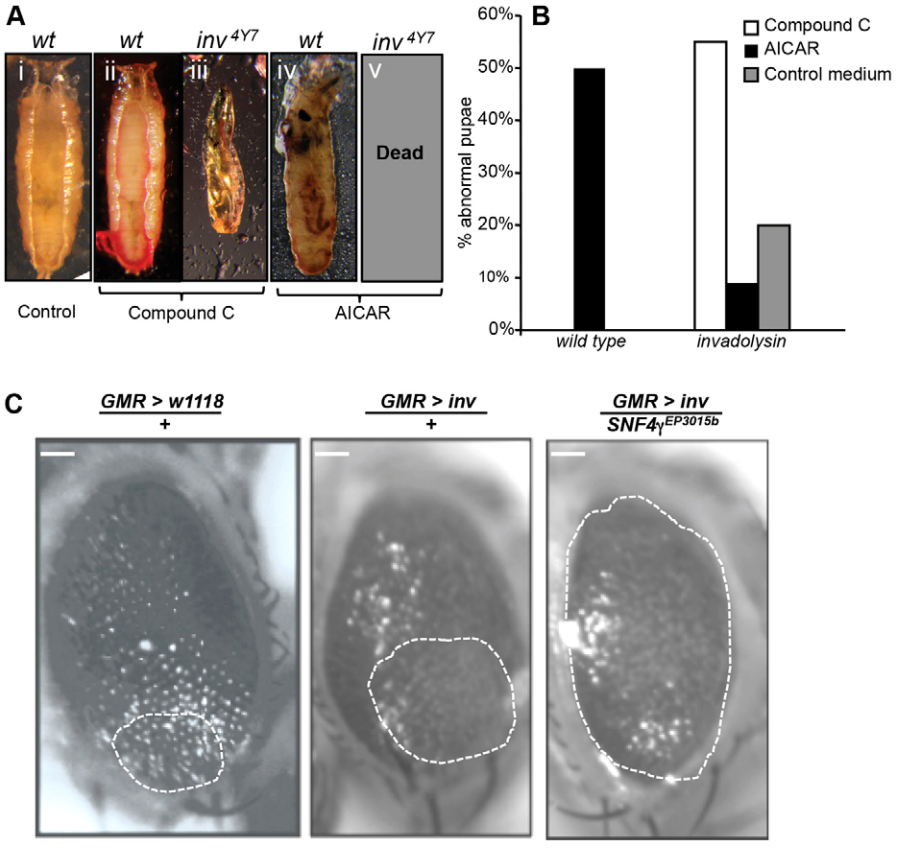


**Fig. 6. Genetic interaction between *invadolysin* and AMPK.** (A) Wild-type (wt) pupae after growth on normal food (i), wild type after growth on food containing the AMPK inhibitor Compound C (ii), $inv^{4Y7}$ after growth on food containing Compound C (iii), wild type pupae after growth on food containing the AMPK activator AICAR (iv), $inv^{4Y7}$ after growth on AICAR (v). (B) Percentage of abnormal pupae in each genotype fed with Compound C, AICAR and normal food. (C) Rough eye phenotype caused by *UAS*-mediated *invadolysin* overexpression under the control of *GMR-Gal4* is enhanced by mutation of $SNF4\gamma^{EP3015b}$. The dashed white circles denote the regions of tissue degradation in the eye. Scale bars: 5 μm.

### Production of ROS is enhanced in mitochondria of *invadolysin* and *bellwether* mutants

Mitochondria play an essential role in generating the majority of cellular ATP, coupling ETC and OXPHOS (oxidative phosphorylation) reactions. During electron transport, mitochondria generate ATP and ROS. ROS encompass a variety of highly reactive metabolites of oxygen including superoxide anions, hydroxyl radicals and hydrogen peroxide (Finkel and Holbrook, 2000). Some of these metabolites are highly unstable whereas others, like hydrogen peroxide, are long-lived. Defects in ETC enzymes increase the cellular production of ROS (Owusu-Ansah et al., 2008). We decided to assess the consequence of reduced mitochondrial ETC activity on the generation of ROS in *invadolysin* mutant larvae. Fat body dissected from *invadolysin, bellwether* and wild-type third-instar larvae was stained with DHE (dihydroethidium), a fluorescent indicator used to analyze the production of ROS *in vivo* (Owusu-Ansah et al., 2008; Robinson et al., 2006). *invadolysin* and *bellwether* fat body showed a more than threefold increase in ROS production, as indicated by strong DHE staining compared to that in wild-type larvae (Fig. 7A,B). We additionally observed a nearly twofold higher accumulation of hydrogen peroxide in *invadolysin* third-instar larvae compared to that in wild-type larvae (Fig. 7C). This suggested that the mitochondrial ETC defects in *invadolysin* mutant animals resulted in an increased accumulation of hydrogen peroxide. We conclude that both *invadolysin* and *bellwether* mutants have defects in mitochondrial ETC activity and thus produce high levels of ROS.

### Increased levels of oxidative damage in *invadolysin larvae*

ROS can damage cellular components (proteins, lipids and DNA), frequently through the formation of carbonyl derivatives (Fridell et al., 2005; Neretti et al., 2009). Increases in ROS are frequently accompanied by an increase in protein carbonyls. As hypothesised, we observed an accumulation in protein carbonyls in $inv^{4Y7}$ larvae compared to wild-type animals (Fig. 7D).

### *invadolysin* larvae are defective in a behavioral response to hypoxia

ROS are not only damaging molecules, but also have an important role in cell signaling (Brookes and Darley-Usmar, 2002; Brookes et al., 2002; Saleh et al., 2008). Mitochondria have

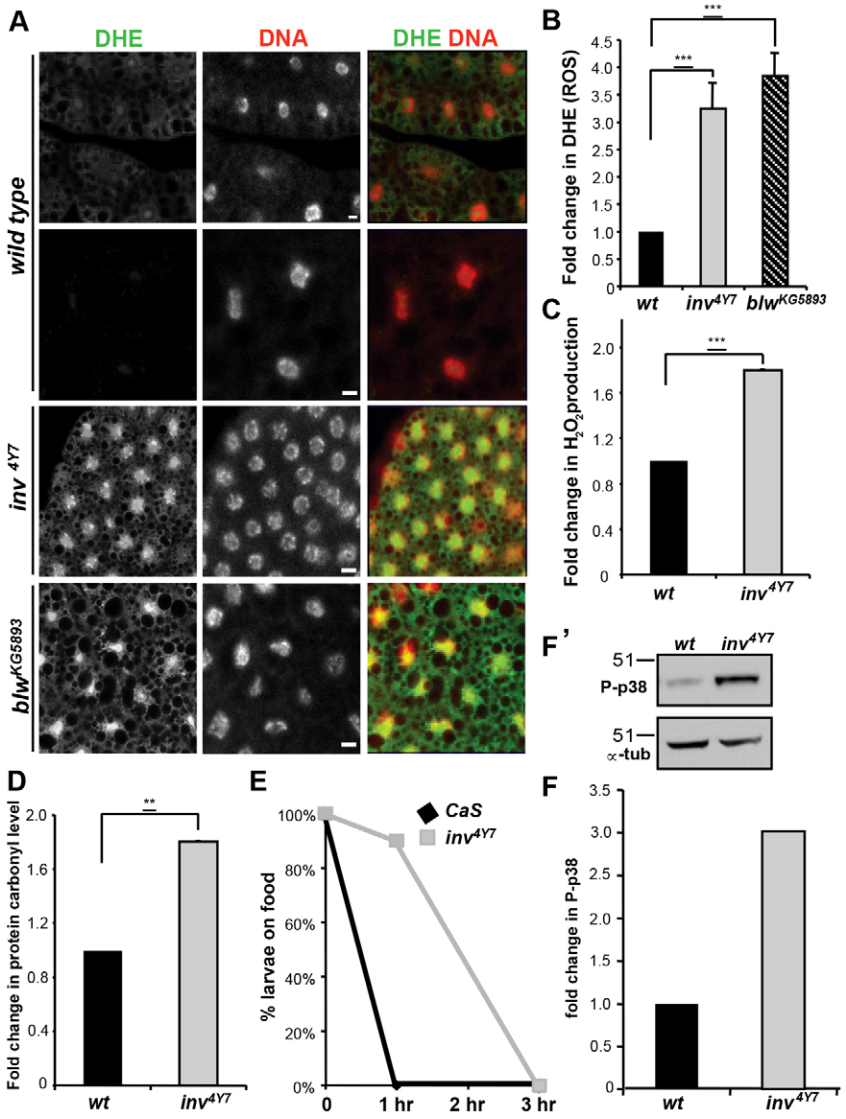


**Fig. 7. Elevated levels of ROS are observed in $inv^{4Y7}$ larvae.** (A) Using dihydroethidium (DHE) to detect ROS in $inv^{4Y7}$ and $blw^{KG5893}$ third-instar larval fat body show elevated ROS compared to wild type. DHE (green), DNA (red) is stained with DAPI. Scale bars: 8 µm. (B) Quantification of the levels of DHE intensity in $inv^{4Y7}$ and $blw^{KG5893}$ third-instar fat body normalized to control tissue (wt). Error bars indicate standard deviation ($n=5$). *invadolysin* mutant larvae show higher levels of (C) hydrogen peroxide and (D) protein oxidation (measured as protein carbonyl) compared to wild-type animals of the same age. Error bars indicate standard deviation ($n=6$). ***$P<0.001$, paired Student's *t*-test. (E) *invadolysin* mutant larvae show an altered behavioral response to hypoxia. In an experiment where the same number of wild-type (CaS) and *invadolysin* larvae were subjected to a hypoxic environment, all wild-type larvae left the yeast paste in the first hour, whereas *invadolysin* larvae only migrated from the yeast paste after 3 hours. (F,F′) Examination of p38 mitogen-activated protein kinase. Immunoblotting of third-instar larval extracts showing phosphorylation status of p38 mitogen-activated protein kinase (P-p38) in *invadolysin* and *bellwether* larvae (F′). Quantification of phosphorylated p38 mitogen-activated protein kinase normalized to α-tubulin levels (F).

been implicated as oxygen sensors (Hagen et al., 2003). In order to regulate oxygen levels in cells, mitochondria increase the generation of ROS to regulate the hypoxia-response mechanism (Chávez et al., 2000). Although *Drosophila* can survive extended periods of hypoxia, hypoxia-response mechanisms cause cell cycle arrest and behavioral changes (Wingrove and O'Farrell, 1999).

In order to test the response of third-instar larvae to conditions of mild hypoxia, $inv^{4Y7}$ and wild-type third-instar larvae were placed in un-crowded conditions on red wine agar plates containing a dollop of yeast paste. The plates were sealed with parafilm to create a mild hypoxic condition. No differences between $inv^{4Y7}$ and wild-type larvae were observed in the first 15 minutes, with both genotypes freely feeding and moving. After 1 hour, we observed that whereas wild-type larvae had stopped feeding and left the yeast paste for the edges of the agar plate, $inv^{4Y7}$ larvae appeared unresponsive to the hypoxic conditions, and were still feeding on the yeast. By 3 hours, all $inv^{4Y7}$ and control larvae had left the central yeast-covered area of the plate (Fig. 7E). Prolonged periods of hypoxia (over 3 hours) resulted in cessation of motility and death of both *invadolysin* and control larvae. These results suggest that the $inv^{4Y7}$ allele affected the short-term 'exploratory' response to hypoxia. One possible explanation for the delay in the response to hypoxia is that lower ATP levels affect the motility of $inv^{4Y7}$ larvae. Another possible explanation is that $inv^{4Y7}$ larvae accumulate higher ROS levels compared to wild type. Higher levels of ROS are required for the transduction of hypoxic signaling. We have shown that ROS levels are consistently high in *invadolysin* larvae (during normoxia) and we therefore suggest that this status could reduce the sensitivity of *invadolysin* larvae to a low oxygen environment, thereby retarding the exploratory response to hypoxia. We observed a threefold higher level of the phosphorylated, active form of p38 in *invadolysin* larvae compared to control animals (Fig. 7F,F′), supporting the hypothesis of a constitutive, activated stress status in $inv^{4Y7}$. p38 mitogen activated protein kinase shows an increased activity in response to environmental stresses such as oxidative stress (Craig et al., 2004).

Changes in gene expression in *invadolysin* mutants support the existence of a 'high stress' condition. We performed microarray studies to investigate the molecular mechanisms by which *invadolysin* regulates energy balance and oxidative responses. RNA extracted from $inv^{4Y7}$ and wild-type third-instar larvae was subjected to microarray analysis (FlyChip service, Cambridge, UK). The microarray results were interpreted using Limma analysis. Analysis of four data sets for each genotype showed that among the 13,817 genes represented on the chip, expression of 231 genes had a decrease of at least 1.5-fold ($P<0.05$) in *invadolysin* larvae, whereas 127 genes showed an increase of at least 1.5-fold ($P<0.05$) in comparison to wild type. DAVID (The Database for Annotation, Visualization and Integrated Discovery) was used to analyze for enrichment of functional categories among the differentially expressed genes, and assess whether the proportion of genes in a gene set representing a functional class (Gene Ontology term, KEGG Pathway) was higher than it would be by chance.

Interestingly, this analysis indicated that the 'defense response' and 'response to stimulus' categories were over-represented in the upregulated gene list, whereas 'mitochondrion', 'lipid particle' and 'ribosomal protein' were enriched in the downregulated gene list (supplementary material Table S3). We observed that ~40% of the upregulated genes fell into categories of defense response and detoxification enzymes, including glutathione S-transferases (*GstD2*, *GstD3*, *GstD6*, *GstD9*) (McElwee et al., 2004) and stress response genes (*thor*). Intriguingly, 58% of the genes downregulated in $inv^{4Y7}$ were nuclear genes encoding mitochondrial proteins, including respiratory chain enzymes (*CoVa*) and mitochondrial ribosomal proteins (*mRpl4*, *mRpl17*) (Liao et al., 2006). Downregulation of genes encoding mitochondrial proteins has been reported as an indication of defects in cell growth and mitochondrial metabolism (Mourikis et al., 2006), a phenotype exhibited by *invadolysin* mutant animals.

The analysis of the transcription profile in *invadolysin* mutants supports the hypothesis that mitochondrial pathways regulating energy production and growth are downregulated when *invadolysin* is mutated. In addition, the reduction in mitochondrial efficiency causes a high-stress status in the developing organism, which is subsequently reflected in the activation of defense response genes.

## Discussion

Our studies demonstrate that the essential metalloproteinase invadolysin interacts with subunits of ATP synthase (Complex V of the mitochondrial respiratory chain) in *Drosophila*.

Invadolysin plays a role in the mitochondrial production of ATP and ROS, possibly through regulating the assembly or activity of ATP synthase. Proteomic analysis has demonstrated that ATP synthase subunits can also be found on lipid droplets from human and mouse adipocytes, *Drosophila* embryos and larval fat body (Beller et al., 2006; Brasaemle et al., 2004; Cermelli et al., 2006; DeLany et al., 2005; Dugail and Hajduch, 2007). We previously reported that human invadolysin localizes to lipid droplets in different human and mouse cell lines (Cobbe et al., 2009). These results suggest that the invadolysin–ATP-synthase interaction might occur on lipid droplets in *Drosophila* and mammalian cells. Interestingly, we also found heat shock cognate protein 3 in samples from both head and larval fat body immunoprecipitates (represented by numerous peptides). Heat shock cognate protein 3 is a member of the heat shock protein family, which has been reported to localize to the endoplasmic reticulum (ER) (Ryoo et al., 2007), as well as on lipid droplets (Beller et al., 2006; Cermelli et al., 2006), and mitochondria (Gallach et al., 2010). Taken together, our experimental results demonstrate an interaction between invadolysin and different mitochondrial proteins, suggesting that *invadolysin* might play a more general role in mitochondrial structure or function.

Increasing evidence has demonstrated that lipid droplets are complex organelles that have multiple cellular functions (Beckman, 2006; Martin and Parton, 2006). Lipid droplets interact with other cellular organelles, including mitochondria (Jägerström et al., 2009). Lipid droplets might work as cellular shuttles for nuclear-encoded mitochondrial proteins, facilitating transport to the mitochondrial compartment following synthesis in the cytoplasm. These subunits could undergo post-translational processing on lipid droplets that might involve modification by invadolysin. Mitochondrial morphogenesis and function depend on a hierarchical network of mechanisms in which proteases appear to be center stage (Guillery et al., 2008; McQuibban et al., 2003; Voos, 2013). Proteases play a pivotal role in mitochondrial gene expression, processing of misfolded and dysfunctional

proteins, mitochondrial lipid metabolism, and fusion of mitochondrial membranes (Anand et al., 2013). We are currently testing the hypothesis that invadolysin might be required for the processing of ATP synthase subunits.

In order to determine whether the physical interaction between invadolysin and ATP synthase subunits was of functional significance, we compared the phenotypes of *invadolysin* and *ATP syn-α* (*bellwether*) mutations. Interestingly, the first *bellwether* mutant allele was isolated during a genetic screen aimed at identifying novel genes involved in growth signaling (Galloni and Edgar, 1999). The phenotype of this allele included larval growth defects affecting all tissues, DNA endoreplication defects and larval lethality. Our previous results demonstrated that larvae homozygous for two *invadolysin* alleles ($inv^{4Y7}$ and $inv^{1}$) presented similar defects. The similarity in the $inv^{4Y7}$ and $blw^{KG5893}$ mutant phenotypes supports the hypothesis that *invadolysin* and *bellwether* function in the same or parallel pathways. This suggestion is also supported by genetic data obtained in an enhancer/suppressor assay, in which we showed that the rough eye phenotype induced by *invadolysin* overexpression was enhanced by the *bellwether* mutation.

### Energy impairment in *invadolysin* larvae

The $inv^{4Y7}$ third-instar larval fat body is smaller, thinner and has a reduced triglyceride content compared to wild-type fat body. We detected similar defects in $blw^{KG5893}$ fat body. Both cell growth and fatty acid synthesis are processes that respond to the energy status of the cell, and are regulated by mitochondria. A reduction in ATP level has been observed in *Drosophila ATP syn-α* mutants (Copeland et al., 2009), and our results revealed that $inv^{4Y7}$ mutant larvae also have a lower ATP content than found in wild-type larvae. ATP is required for many essential processes during development, including transcriptional regulation (e.g. histone modification) and cell migration (Le Clainche and Carlier, 2008; Lee et al., 2005; Saxton et al., 1988). We have previously shown that germ cell migration is defective in *invadolysin* mutant embryos (McHugh et al., 2004). Cell migration requires actin treadmilling, which, in turn, is a bioenergetically demanding process that hydrolyses ATP (Le Clainche and Carlier, 2008). A reduction in ATP content might explain the germ cell migration defect observed in the *invadolysin* mutant.

AMPK acts as an energy sensor to regulate cell growth and the cell cycle in invertebrates and vertebrates alike (Hardie, 2004; Hardie, 2005; Mandal et al., 2005). During metabolic stress, ATP consumption is increased, raising AMP levels. Increased AMP leads to the phosphorylation and activation of AMPK (Pan and Hardie, 2002). AMPK-null mutants die with cell polarity and mitotic defects in embryonic cells and larval neuroblasts (Lee et al., 2007). We have demonstrated that $inv^{4Y7}$ larvae have reduced levels of ATP and a hyper-activation of AMPK (as shown by elevated phosphorylation). The correlation between the $inv^{4Y7}$ mutation and AMPK activation is confirmed by genetic interaction, whereby the rough-eye phenotype caused by overexpression of *invadolysin* is enhanced by mutation in *SNF4γ*, the AMP-sensor subunit of AMPK. Our data suggest that AMPK might play an antagonistic role to invadolysin. Strikingly, $inv^{4Y7}$ larvae fed Compound C, an AMPK inhibitor, exhibited longer larval life and even formed pupae (which fail to eclose due to a lack of imaginal discs) – in effect, a partial rescue. This effect was not observed in wild-type animals fed Compound C. The development of $inv^{4Y7}$ on food supplemented with AICAR, an AMPK activator, did not alter the $inv^{4Y7}$ phenotype, yet it deleteriously affected pupal development and viability of wild-type animals. These data led us to hypothesize that AMPK is activated in response to the stress caused by the mutation of $inv^{4Y7}$, which in turn contributes to larval lethality.

Under conditions of energy depletion, AMPK responds by inhibiting anabolic reactions and accelerating catabolic pathways. ACC, one of the substrates for AMPK (Ha et al., 1994), is involved in fatty acid synthesis. Phosphorylation of ACC by AMPK inhibits ACC activity. The phosphorylation level of ACC in *invadolysin* larvae was significantly higher than in wild-type larvae, suggesting decreased ACC activity that is consistent with our observation of lower triglyceride content in larvae lacking invadolysin.

### Loss of *invadolysin* affects mitochondrial membrane potential

A decrease of ATP synthesis is normally associated with a reduction in mitochondrial membrane potential (Sugiyama et al., 2007). It has been reported, in *Drosophila* (Copeland et al., 2009) and in humans (Celotto et al., 2006), that mutations affecting ATP synthase genes alter the mitochondrial membrane potential. We found that mitochondria in both *invadolysin* and *bellwether* third-instar larval fat body have reduced mitochondrial membrane potential compared to that of wild-type larvae. However, based on a quantification of mitochondrial:nuclear DNA, the overall density of mitochondria does not appear to be different in mutant larvae. The alteration of mitochondrial membrane potential suggests that $inv^{4Y7}$ affects ATP synthesis. A reduction in mitochondrial membrane potential has also been observed in mutations for other mitochondrial proteins (Galloni, 2003), corroborating our hypothesis that *invadolysin* is involved in mitochondrial regulation.

Mutations in ATP synthase genes are associated with alteration of mitochondrial morphology in *Drosophila* neurons and flight muscles, rat and mouse liver cells, beef heart, HeLa cells, *Caenorhabditis elegans* and *Chaos carolinensis* (Celotto et al., 2006; Mannella, 2008). Measurement of mitochondria in $inv^{4Y7}$ and $blw^{KG5893}$ fat body demonstrated an alteration in mitochondrial shape and size compared to that of wild-type cells. Mitochondria are dynamic organelles, and their size and inner membrane organization are frequently modified in response to the physiological status of cells.

Defects in respiratory chain enzymes can also create an accumulation of ROS and a corresponding increase in oxidative stress (Bell et al., 2007). Under normal metabolic conditions, ROS play a role as second messengers in signal transduction (Brookes and Darley-Usmar, 2002). ROS generated by the mitochondrial ETC have been shown to play a role in regulating the cell cycle, apoptosis, response to hypoxia, modification of lipid metabolism and mitochondrial protein expression (Brookes et al., 2002; Curtis et al., 2007; Owusu-Ansah et al., 2008; Xie and Roy, 2012). Loss of *invadolysin* enhances ROS production and exacerbates oxidative stress. It has also been reported that increased formation of oxygen radicals increases oxidative stress in the ATP synthase subunit α (ATP5a1) mutant rat. (Saleh et al., 2008).

We observed elevated levels of ROS in *invadolysin* and *bellwether* mutant third-instar larvae. We additionally established that *invadolysin* mutants accumulate a high amount of hydrogen peroxide and show oxidative damage in the form of protein carbonyls. Generally, elevated levels of ROS produced by the mitochondrial respiratory chain under conditions of stress (such

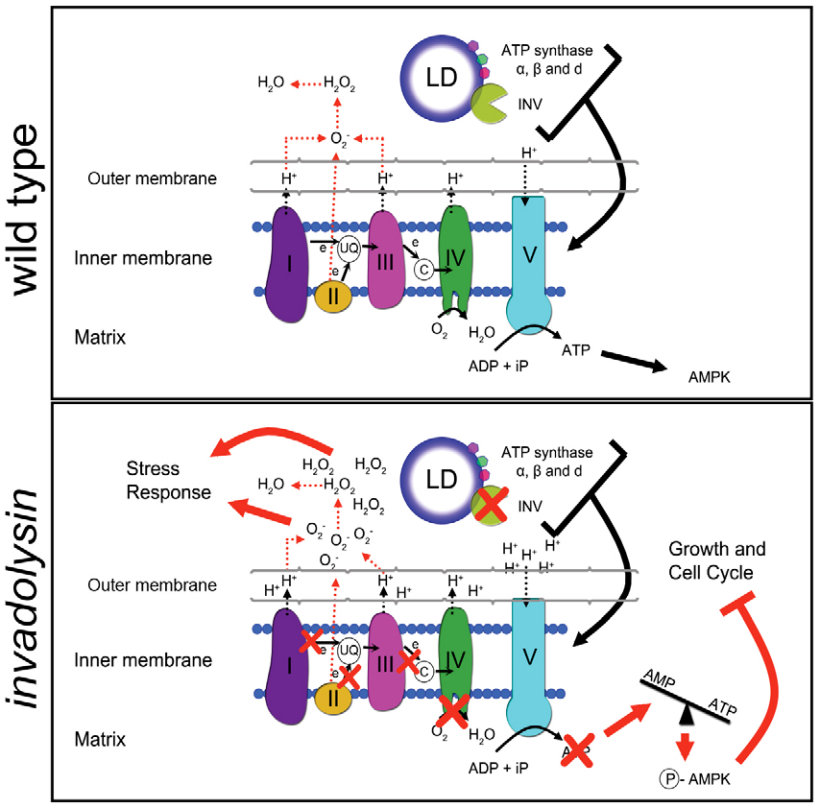


**Fig. 8. Model showing the role and effect of invadolysin on the ETC.** Schematic representation of the ETC and lipid droplets. The top box represents a normal wild-type organism, whereas the lower box represents the effects observed upon mutation of *invadolysin*. In the *invadolysin* mutant, the ETC is disrupted, resulting in an accumulation of ROS, a reduction in ATP synthesis, cell cycle arrest, growth defects and an activated stress response. This results in organism death. I–V, complexes I–V; UQ, ubiquinone; C, cytochrome *c*, iP, inorganic phosphate.

as hypoxia) signal the activation of the stress response pathway, but only once a critical ROS threshold is reached (Bell et al., 2007). We observed that $inv^{4Y7}$ larvae have a slower behavioral response to hypoxia as compared to wild-type animals. One possible explanation is that stress responses are constitutively activated even under normal physiological conditions in *invadolysin* larvae (which show elevated levels of ROS), and mutant larvae are thus less able to sense changes to oxygen level in the environment. Genome-wide expression analysis supports this hypothesis, as there are higher levels of transcripts for genes involved in defense responses (e.g. heat shock and GST proteins) in *invadolysin* mutant larvae.

Taken together, our data demonstrate that *invadolysin* is important for the normal activity of mitochondria, and consequently modulation of energy balance and the oxidative stress response – processes essential in controlling crucial developmental events such as cell growth and the cell cycle (Owusu-Ansah et al., 2008).

## Conclusions and model of invadolysin action

On the basis of the results of this study, we postulate that invadolysin has a role in the formation or function of the ETC. We hypothesize that invadolysin is required for the correct processing of the ATP synthase complex during its biosynthesis, transport and/or assembly. As a consequence, the flux of the ETC is not as efficient in the absence of invadolysin as it is in control animals. Lower levels of ATP in *invadolysin* mutant animals result in a block to anabolic pathways, such as fatty acid synthesis. The lower concentration of cellular ATP affects the energy status of the organism, and might also contribute to the cell cycle and cell migration defects observed in *invadolysin* mutant larvae. Defects in the ETC also cause an accumulation in cellular ROS. This high concentration of ROS, in particular hydrogen peroxide, causes cellular damage and affects stress response pathways (Fig. 8).

In conclusion, we discovered a pivotal role for invadolysin, a novel essential metalloproteinase, in maintaining mitochondrial functionality. We established that invadolysin is required for mitochondrial metabolism and maintaining the correct energetic and redox status in the cell. Given the conservation of *invadolysin*, we speculate that a similar function will also exist in higher metazoa.

## Materials and Methods

### *Drosophila* husbandry and lines

Fly stocks were maintained at 25°C on standard cornmeal medium, unless otherwise noted. $inv^{4Y7}$ was generated by local hopping of a nearby P transposon insertion, *l(3)04017*, obtained from the Bloomington Stock Center (described in McHugh et al., 2004). UAS-HA-invadolysin-cDNA flies were generated as described below. *Canton S* was utilized as the control wild-type strain (Celotto et al., 2006). All other stocks were obtained from the Bloomington Stock Center.

### Molecular cloning

*Drosophila* EST clone 5168166 was sequenced and the full-length coding sequence for *invadolysin* was amplified by PCR and cloned into the pUAST vector (the GenBank accession number for invadolysin full-length cDNA is AE014297.2). The hemagglutinin tag epitope (HA) sequence (5′-TACCCATA-CGATGTTCCAGATTACGCT-3′ or 5′-TATCCATATGATGTTCCAGATTAT-GCT-3′) was amplified by PCR and then cloned into the invadolysin coding sequence (nt 242–247) in pUAST.

### Immunoprecipitation from adult heads and larval fat body

Heads were removed from 100 3-day-old adult *GMR-Gal4>UAS-HA-inv* and wild-type flies. Alternatively, fat body tissue was dissected from 100 well-fed third-instar *cg-Gal4>UAS-HA-inv* and wild-type larvae. Heads or fat body were homogenized in 500 µl of cold lysis buffer (20 mM Tris-HCl pH 8, 100 mM NaCl, 0.1% Nonidet P40) containing Complete protease inhibitor cocktail (Roche). 100 µl of resuspended anti-HA Affinity Matrix (Roche) was added to each tube of lysate and incubated at 4°C for 2 hours. The matrix was washed three times in lysis

buffer and then resuspended in 75 µl electrophoresis sample buffer (20 mM Tris-HCl pH 7.5, 2 mM EDTA, 5% SDS, 0.02% Bromophenol Blue, 20% glycerol, 200 mM DTT) and boiled for 10 minutes. 50% of each sample was analyzed by immunoblotting to ensure successful immunopurification of HA–invadolysin. The remaining 50% of the sample was resolved on precast 4–12% Bis-Tris polyacrylamide gels (Novex) and stained with colloidal Coomassie Blue (Invitrogen). Regions of interest at comparable molecular mass were excised from each lane (HA–invadolysin and wild-type immunopurified samples) and mass spectrometric analysis was performed (Conway Institute, University College Dublin, Ireland).

#### Mass spectrometry

Mass spectrometry was performed as reported previously (Bolukbasi et al., 2012). The proteins, in slices from SDS–PAGE gels, were digested in-gel with trypsin by the method of Shevchenko et al. (Shevchenko et al., 1996). The resulting peptide mixtures were resuspended in 1% formic acid and analyzed by nanoelectrospray liquid chromatography tandem mass spectrometry (nano-LC-MS/MS). A high performance liquid chromatography (HPLC) instrument (Dionex, UK) was interfaced with an LTQ ion trap mass spectrometer (Thermo Finnigan, CA). Chromatography buffer solutions (buffer A: 5% acetonitrile and 0.1% formic acid; buffer B: 80% acetonitrile and 0.1% formic acid) were used to deliver a 60-minute gradient (35 minutes to 45% buffer B, 10 minutes to 90%, hold 10 minutes, 3 minutes to 5% and hold for 15 minutes). A flow rate of 2 µl per minute was used at the electrospray source. One full scan was followed by ten MS/MS events, and the duty cycle programmed to enforce dynamic exclusion for 2 minutes. MS/MS spectra were searched using the Sequest algorithm against the SwissProt.2007.04.19 database restricted to *Drosophila melanogaster* entries. The settings used were: parent ion tolerance (2.0 Da); CID fragment ion tolerance (1.0 Da); semi-tryptic cleavage (one or fewer missed cleavages permitted); fixed modification (carboxymethyl cysteine +58.005); dynamic modification (oxidized methionine +15.995). The FDR was estimated at $<1\%$ using the PeptideProphet program. Proteins with a ProteinProphet probability score $>0.99$ identified by a minimum of two different peptide spectra were deemed identified, additionally all spectra of identified proteins were manually checked for quality.

#### Nile Red staining and Triacylglycerol assay of fat body

Third-instar larval fat body staining with the lipophilic reagent Nile Red and larval triglyceride level measurement were performed as described previously (Cobbe et al., 2009).

#### Larval MitoTracker, JC-1 and DHE staining

##### Mitotracker Red (active mitochondria)

Larvae of the same stage and the appropriate genotype were dissected in PBS directly on a glass slide and the fat body was isolated and immediately fixed with 4% paraformaldehyde (Thermo Scientific) in PBS. The tissue was then washed three times with PBS plus 1% Tween-20 (PBS-Tw) for 10 minutes each. Tissue was stained in PBS-Tw containing 300 nM Mitotracker Red (Molecular Probes) and 1 µg/ml DAPI (Sigma) for 30 minutes, followed by six 10-minute washes with PBS-Tw. The tissue was mounted in 90% glycerol.

##### JC-1 (all mitochondria)

To visualize the mitochondria, fat body from larvae of the appropriate genotype was dissected in Schneider's insect medium (Sigma) directly on a glass slide. The fat body was washed twice in double-distilled $H_2O$ and stained with 5 µg/ml JC-1 (Molecular Probes) and 1 µg/ml DAPI (Sigma) in double-distilled $H_2O$ for 15 minutes. The tissue was washed twice in double-distilled $H_2O$ followed by three 5-minute washes with Schneider's insect medium. Tissue was then mounted in 90% glycerol.

##### DHE (ROS assay)

Larvae of the same stage and the appropriate genotype were dissected in PBS directly on a glass slide and the fat body was isolated followed by DHE (dihydroethidium, Molecular Probes) staining as described previously (Owusu-Ansah et al., 2008).

#### Behavioral assay for hypoxia response

The hypoxia-induced motility assay was performed on late third-instar larvae. Well-fed third-instar larvae were transferred in uncrowded conditions to yeast paste in the middle of a 10-cm red wine agar plate. The larvae were allowed to settle for about 10 minutes. Plates were then sealed with parafilm and incubated at room temperature from 4–12 hours. Motility was scored as frequency of larvae that moved to the edge of the plate, and was plotted as a function of time.

#### Compound C and AICAR treatments on developing *Drosophila*

Wild-type and $inv^{4Y7}$ flies were left to mate on standard medium and medium supplemented with 1 mg/ml (5 mM) AICAR (Cell Signaling) or 20 mg/ml (0.2 mM) Compound C (MERCK) for 24 hours and then discarded. The effect of the drugs on the development of each genotype was compared to animals fed on regular medium. Every experiment was performed in triplicate. The results plotted are reported as the percentage of abnormal pupae that developed within 15 days on each medium.

#### ATP assay

Wild-type and $inv^{4Y7}$ larvae were grown on fresh yeast paste on red wine agar plates. Six wild-type or 24 $inv^{4Y7}$ larvae were rinsed in PBS and then homogenized with a motorized pestle in mitochondrial buffer (250 mM sucrose, 5 mM Tris-HCl pH 7.4, 2 mM EGTA, 1% BSA at 4°C) (Miwa and Brand, 2003) and immediately centrifuged at 12,000 rpm in an Eppendorf centrifuge for 10 minutes. 10 µl of the supernatant was used for ATP measurement using an ATP determination kit (Molecular Probe). Total ATP was normalized to total protein (determined using a Bradford protein assay) from third-instar larvae. Because the isolation medium contained BSA, the protein concentration in the isolation medium was subtracted from the samples. All analyses were performed in triplicate. Statistical analysis was performed using the Student's *t*-test.

#### Hydrogen peroxide and protein carbonyl measurement

Wild-type and $inv^{4Y7}$ third-instar larvae were homogenized in mitochondrial buffer as described above. Hydrogen peroxide production was measured using the Amplex Red kit (Molecular Probes). Hydrogen peroxide levels were normalized to total protein (determined using a Bradford protein assay). Because the isolation medium contained BSA, the protein concentration in the isolation medium was subtracted from the samples. Protein carbonyl concentration was determined using the OxiSelect Protein Carbonyl ELISA kit (Cell Biolabs) following the protocol provided by the manufacturer. All analyses were performed in triplicate. Statistical analysis was performed using the Student's *t*-test.

#### RNA extraction and qPCR

RNA extraction and cDNA synthesis were performed as described in (Bolukbasi et al., 2012). Quantitative real-time PCR (qPCR) was performed using the Lightcycler® 480 Real-time PCR system (Roche), Lightcycler® 480 probes master mix (Roche) and the Roche Universal Probe Library assay. Probe #89 together with oligonucleotides *inv-F* (5′-GCTCTTGGCTCCTCGTTTC-3′) and *inv-R* (5′-TCTTCGCTATCAGCCAGTTG-3′) were used to amplify the *invadolysin* transcript. Probe #3 together with oligonucleotides *blw-F* (5′-TCGGTTC-CGATCTGGATG-3′) and *blw-R* (5′-GCACACCGCAGTAGATAACG-3′) were used to detect the *bellwether* transcript. Probe #151 (04694376001) together with oligonucleotides *CoI-F* (5′-TGGAGCTGGAACAGGATGAAC-3′) and *CoI-R* (5′-CAACTGAAGCTCCACCATGA-3′) were used to amplify the mitochondrial *cytochrome oxidase subunit I* (*CoI*). Probe #132 (04694163001) and oligonucleotides *Act5C-F* (5′-AGACACCAAACCGAAAGACTTAAT-3′) and *Act5C-R* (5′-ACATGCCAGAGCCGTTGT-3′) were used to amplify nuclear *actin 5C*. Actin 5C was used as control to normalize equal loading of template cDNA.

#### Mitochondrial DNA:nuclear DNA ratio

The relative mitochondrial DNA:nuclear DNA ratio was determined by the ratio of the number of copies for mitochondrial *CoI* to that of nuclear *actin 5C* (Neretti et al., 2009). DNA was extracted from six third-instar larvae using the mitochondrial QiAmp DNA Micro Kit (QIAGEN). DNA copy number was determined using qPCR as described above.

#### Microarray

Gene expression analysis was performed as reported previously (Bolukbasi et al., 2012). Microarray data were deposited in the Gene Expression Omnibus (http://www.ncbi.nlm.nih.gov/geo/) with accession number GSE41029.

#### Preparation of larval protein extracts and immunoblotting

The procedure was performed as previously described (Bolukbasi et al., 2012; Cobbe et al., 2009). Primary antibody dilutions used in the immunoblotting experiments were as follows: rat HA antibody (Roche, used at 1:500), AMPK and phospho-AMPK (Cell Signaling Technology, used at 1:500), phospho-p38 (Cell Signaling Technology, used at 1:500), ACC1 (Cell Signaling Technology, used at 1:500), phospho-ACC-1 (Kinasource Ltd, used at 1:500). Appropriate IRDye 700 and 800 secondary antibodies were used at 1:10,000. Blots were scanned with the Odyssey Infrared Imaging System (LI-COR Biosciences).

#### Microscopy

Light microscopy images of *Drosophila* adult eyes were captured on an Olympus SZX7 dissection microscope fitted with an Olympus SP-500UZ digital camera. The images were processed using Adobe Photoshop CS.

OPTIGrid microscopy analysis of fat body was performed as reported previously (Cobbe et al., 2009).

Confocal microscopy was performed by imaging sample on a Leica Confocal SP5, with an inverted DMI 6000 CS microscope base and equipped with three

photomultiplier tubes (Hamamatsu R 9624). The images were captured using the Leica application suite – advanced fluorescence (Version 2.0.0, build 1934). Quantification of intensity was performed using Volocity (Version 5.03, Build 4) 'find objects by intensity' (taking half the maximum intensity as threshold), 'exclude objects by size' ($<1\ \mu m^2$) and 'measure object' tools. The average mean intensity of every object was quantified and normalized to wild type, which was set at a value of one. *P*-values were calculated using the paired Student's *t*-test and the standard deviation of each group was obtained. For the mitochondrial measurements, z-stacks were captured at 167.7 nm sections using a 40× oil objective and 117.8 nm sections with a 100× oil objective. The *z*-stacks were deconvolved using Huygens Essential software (Scientific Volume Imaging). Measurements were taken using the line measure tool in Volocity. P-values were calculated using the paired Student's *t*-test and the standard deviation of each group was obtained.

For scanning electron microscopy (SEM), fly heads removed from 1–5-day-old fly heads were fixed in 3% glutaraldehyde in 0.1 M sodium cacodylate buffer, pH 7.3, for 2–3 hours. Samples were then washed three times for 10 minutes each time in 0.1 M sodium cacodylate buffer. Specimens were then post-fixed in 1% osmium tetroxide in 0.1 M sodium cacodylate buffer for 45 minutes, prior to being washed with three 10 minute changes of 0.1 M sodium cacodylate buffer. The samples were then dehydrated in 50%, 70%, 90% and 100% normal grade acetone for 10 minutes each, then for a further two 10 minutes changes in acetone analaR. Dehydrated samples were then critical-point dried, mounted on aluminum stubs, sputter coated with gold palladium and viewed in a Philips SEM 505. Areas of interest were photographed on black-and-white negative film. Images were processed using Adobe Photoshop CS.

## Acknowledgements

The authors wish to acknowledge the ongoing, superb efforts of both the Bloomington *Drosophila* Stock Centre and FlyBase (a database of *Drosophila* genes and genomes) without which much of the insights made in this study would not have been possible.

## Author contributions

F.D. designed most of the experiments, performed the immunoprecipitation, ATP, protein carbonyl and ROS assays and immunoblot analyses, and prepared the first draft of the manuscript. E.D. performed the microscopy analysis, triglyceride assay and lipid staining, and assisted in editing the manuscript. F.D. and E.D. cooperated in the molecular cloning of tagged proteins, and molecular and genetic analyses. D.R.D. performed the microarray statistical analysis. G.C. carried out the mass spectrometry analysis. M.M.S.H. conceived the study and coordinated the project with F.D., and helped to write the final manuscript. All authors approved the final manuscript.

## Funding

F.D.C. was supported by an award from the Norman Salvesen Emphysema Research Trust while at the University of Edinburgh. E.D. was funded by a PhD studentship from the University of Edinburgh, College of Medicine and Veterinary Medicine. M.H. and the research in the Heck laboratory was supported by a Wellcome Trust University Award, and a Wellcome Trust Project grant. D.R.D. was funded by a British Heart Foundation Centre for Research Excellence award. Deposited in PMC for release after 6 months.

Supplementary material available online at
http://jcs.biologists.org/lookup/suppl/doi:10.1242/jcs.133306/-/DC1

## References

**Ackerman, S. H. and Tzagoloff, A.** (2005). Function, structure, and biogenesis of mitochondrial ATP synthase. *Prog. Nucleic Acid Res. Mol. Biol.* **80**, 95-133.

**Anand, R., Langer, T. and Baker, M. J.** (2013). Proteolytic control of mitochondrial function and morphogenesis. *Biochim. Biophys. Acta* **1833**, 195-204.

**Beckman, M.** (2006). Cell biology. Great balls of fat. *Science* **311**, 1232-1234.

**Bell, E. L., Klimova, T. A., Eisenbart, J., Moraes, C. T., Murphy, M. P., Budinger, G. R. and Chandel, N. S.** (2007). The Qo site of the mitochondrial complex III is required for the transduction of hypoxic signaling via reactive oxygen species production. *J. Cell Biol.* **177**, 1029-1036.

**Bellen, H. J., Levis, R. W., Liao, G., He, Y., Carlson, J. W., Tsang, G., Evans-Holm, M., Hiesinger, P. R., Schulze, K. L., Rubin, G. M. et al.** (2004). The BDGP gene disruption project: single transposon insertions associated with 40% of Drosophila genes. *Genetics* **167**, 761-781.

**Beller, M., Riedel, D., Jänsch, L., Dieterich, G., Wehland, J., Jäckle, H. and Kühnlein, R. P.** (2006). Characterization of the Drosophila lipid droplet subproteome. *Mol. Cell. Proteomics* **5**, 1082-1094.

**Bolukbasi, E., Vass, S., Cobbe, N., Nelson, B., Simossis, V., Dunbar, D. R. and Heck, M. M.** (2012). Drosophila poly suggests a novel role for the Elongator complex in insulin receptor-target of rapamycin signalling. *Open Biol.* **2**, 110031.

**Brand, A. H. and Perrimon, N.** (1993). Targeted gene expression as a means of altering cell fates and generating dominant phenotypes. *Development* **118**, 401-415.

**Brasaemle, D. L., Dolios, G., Shapiro, L. and Wang, R.** (2004). Proteomic analysis of proteins associated with lipid droplets of basal and lipolytically stimulated 3T3-L1 adipocytes. *J. Biol. Chem.* **279**, 46835-46842.

**Brookes, P. and Darley-Usmar, V. M.** (2002). Hypothesis: the mitochondrial NO(*) signaling pathway, and the transduction of nitrosative to oxidative cell signals: an alternative function for cytochrome C oxidase. *Free Radic. Biol. Med.* **32**, 370-374.

**Brookes, P. S., Levonen, A. L., Shiva, S., Sarti, P. and Darley-Usmar, V. M.** (2002). Mitochondria: regulators of signal transduction by reactive oxygen and nitrogen species. *Free Radic. Biol. Med.* **33**, 755-764.

**Celotto, A. M., Frank, A. C., McGrath, S. W., Fergestad, T., Van Voorhies, W. A., Buttle, K. F., Mannella, C. A. and Palladino, M. J.** (2006). Mitochondrial encephalomyopathy in Drosophila. *J. Neurosci.* **26**, 810-820.

**Cermelli, S., Guo, Y., Gross, S. P. and Welte, M. A.** (2006). The lipid-droplet proteome reveals that droplets are a protein-storage depot. *Curr. Biol.* **16**, 1783-1795.

**Chacinska, A., Koehler, C. M., Milenkovic, D., Lithgow, T. and Pfanner, N.** (2009). Importing mitochondrial proteins: machineries and mechanisms. *Cell* **138**, 628-644.

**Chávez, J. C., Agani, F., Pichiule, P. and LaManna, J. C.** (2000). Expression of hypoxia-inducible factor-1alpha in the brain of rats during chronic hypoxia. *J. Appl. Physiol.* **89**, 1937-1942.

**Cobbe, N., Marshall, K. M., Gururaja Rao, S., Chang, C. W., Di Cara, F., Duca, E., Vass, S., Kassan, A. and Heck, M. M.** (2009). The conserved metalloprotease invadolysin localizes to the surface of lipid droplets. *J. Cell Sci.* **122**, 3414-3423.

**Copeland, J. M., Cho, J., Lo, T., Jr, Hur, J. H., Bahadorani, S., Arabyan, T., Rabie, J., Soh, J. and Walker, D. W.** (2009). Extension of Drosophila life span by RNAi of the mitochondrial respiratory chain. *Curr. Biol.* **19**, 1591-1598.

**Craig, C. R., Fink, J. L., Yagi, Y., Ip, Y. T. and Cagan, R. L.** (2004). A Drosophila p38 orthologue is required for environmental stress responses. *EMBO Rep.* **5**, 1058-1063.

**Curtis, C., Landis, G. N., Folk, D., Wehr, N. B., Hoe, N., Waskar, M., Abdueva, D., Skvortsov, D., Ford, D., Luu, A. et al.** (2007). Transcriptional profiling of MnSOD-mediated lifespan extension in Drosophila reveals a species-general network of aging and metabolic genes. *Genome Biol.* **8**, R262.

**DeLany, J. P., Floyd, Z. E., Zvonic, S., Smith, A., Gravois, A., Reiners, E., Wu, X., Kilroy, G., Lefevre, M. and Gimble, J. M.** (2005). Proteomic analysis of primary cultures of human adipose-derived stem cells: modulation by Adipogenesis. *Mol. Cell. Proteomics* **4**, 731-740.

**Devenish, R. J., Prescott, M. and Rodgers, A. J.** (2008). The structure and function of mitochondrial F1F0-ATP synthases. *Int. Rev. Cell Mol. Biol.* **267**, 1-58.

**Dugail, I. and Hajduch, E.** (2007). A new look at adipocyte lipid droplets: towards a role in the sensing of triacylglycerol stores? *Cell. Mol. Life Sci.* **64**, 2452-2458.

**Finkel, T. and Holbrook, N. J.** (2000). Oxidants, oxidative stress and the biology of ageing. *Nature* **408**, 239-247.

**Fridell, Y. W., Sánchez-Blanco, A., Silvia, B. A. and Helfand, S. L.** (2005). Targeted expression of the human uncoupling protein 2 (hUCP2) to adult neurons extends life span in the fly. *Cell Metab.* **1**, 145-152.

**Gallach, M., Chandrasekaran, C. and Betrán, E.** (2010). Analyses of nuclearly encoded mitochondrial genes suggest gene duplication as a mechanism for resolving intralocus sexually antagonistic conflict in Drosophila. *Genome Biol. Evol.* **2**, 835-850.

**Galloni, M.** (2003). Bonsaï, a ribosomal protein S15 homolog, involved in gut mitochondrial activity and systemic growth. *Dev. Biol.* **264**, 482-494.

**Galloni, M. and Edgar, B. A.** (1999). Cell-autonomous and non-autonomous growth-defective mutants of Drosophila melanogaster. *Development* **126**, 2365-2375.

**Guillery, O., Malka, F., Landes, T., Guillou, E., Blackstone, C., Lombès, A., Belenguer, P., Arnoult, D. and Rojo, M.** (2008). Metalloprotease-mediated OPA1 processing is modulated by the mitochondrial membrane potential. *Biol. Cell* **100**, 315-325.

**Ha, J., Daniel, S., Broyles, S. S. and Kim, K. H.** (1994). Critical phosphorylation sites for acetyl-CoA carboxylase activity. *J. Biol. Chem.* **269**, 22162-22168.

**Hagen, T., Taylor, C. T., Lam, F. and Moncada, S.** (2003). Redistribution of intracellular oxygen in hypoxia by nitric oxide: effect on HIF1alpha. *Science* **302**, 1975-1978.

**Hardie, D. G.** (2004). The AMP-activated protein kinase pathway – new players upstream and downstream. *J. Cell Sci.* **117**, 5479-5487.

**Hardie, D. G.** (2005). New roles for the LKB1—>AMPK pathway. *Curr. Opin. Cell Biol.* **17**, 167-173.

**Inoki, K., Zhu, T. and Guan, K. L.** (2003). TSC2 mediates cellular energy response to control cell growth and survival. *Cell* **115**, 577-590.

**Jägerström, S., Polesie, S., Wickström, Y., Johansson, B. R., Schröder, H. D., Højlund, K. and Boström, P.** (2009). Lipid droplets interact with mitochondria using SNAP23. *Cell Biol. Int.* **33**, 934-940.

**Lai-Zhang, J., Xiao, Y. and Mueller, D. M.** (1999). Epistatic interactions of deletion mutants in the genes encoding the F1-ATPase in yeast Saccharomyces cerevisiae. *EMBO J.* **18**, 58-64.

**Le Clainche, C. and Carlier, M. F.** (2008). Regulation of actin assembly associated with protrusion and adhesion in cell migration. *Physiol. Rev.* **88**, 489-513.
**Lee, D., Ezhkova, E., Li, B., Pattenden, S. G., Tansey, W. P. and Workman, J. L.** (2005). The proteasome regulatory particle alters the SAGA coactivator to enhance its interactions with transcriptional activators. *Cell* **123**, 423-436.
**Lee, J. H., Koh, H., Kim, M., Kim, Y., Lee, S. Y., Karess, R. E., Lee, S. H., Shong, M., Kim, J. M., Kim, J. et al.** (2007). Energy-dependent regulation of cell structure by AMP-activated protein kinase. *Nature* **447**, 1017-1020.
**Li, W. Z., Li, S. L., Zheng, H. Y., Zhang, S. P. and Xue, L.** (2012). A broad expression profile of the GMR-GAL4 driver in Drosophila melanogaster. *Genet. Mol. Res.* **11**, 1997-2002.
**Liao, T. S., Call, G. B., Guptan, P., Cespedes, A., Marshall, J., Yackle, K., Owusu-Ansah, E., Mandal, S., Fang, Q. A., Goodstein, G. L. et al.** (2006). An efficient genetic screen in Drosophila to identify nuclear-encoded genes with mitochondrial function. *Genetics* **174**, 525-533.
**Lippai, M., Csikós, G., Maróy, P., Lukácsovich, T., Juhász, G. and Sass, M.** (2008). SNF4Agamma, the Drosophila AMPK gamma subunit is required for regulation of developmental and stress-induced autophagy. *Autophagy* **4**, 476-486.
**Mandal, S., Guptan, P., Owusu-Ansah, E. and Banerjee, U.** (2005). Mitochondrial regulation of cell cycle progression during development as revealed by the tenured mutation in Drosophila. *Dev. Cell* **9**, 843-854.
**Mannella, C. A.** (2008). Structural diversity of mitochondria: functional implications. *Ann. N. Y. Acad. Sci.* **1147**, 171-179.
**Martin, S. and Parton, R. G.** (2006). Lipid droplets: a unified view of a dynamic organelle. *Nat. Rev. Mol. Cell Biol.* **7**, 373-378.
**McBride, H. M., Neuspiel, M. and Wasiak, S.** (2006). Mitochondria: more than just a powerhouse. *Curr. Biol.* **16**, R551-R560.
**McElwee, J. J., Schuster, E., Blanc, E., Thomas, J. H. and Gems, D.** (2004). Shared transcriptional signature in Caenorhabditis elegans Dauer larvae and long-lived daf-2 mutants implicates detoxification system in longevity assurance. *J. Biol. Chem.* **279**, 44533-44543.
**McHugh, B., Krause, S. A., Yu, B., Deans, A. M., Heasman, S., McLaughlin, P. and Heck, M. M.** (2004). Invadolysin: a novel, conserved metalloprotease links mitotic structural rearrangements with cell migration. *J. Cell Biol.* **167**, 673-686.
**McQuibban, G. A., Saurya, S. and Freeman, M.** (2003). Mitochondrial membrane remodelling regulated by a conserved rhomboid protease. *Nature* **423**, 537-541.
**Miwa, S. and Brand, M. D.** (2003). Mitochondrial matrix reactive oxygen species production is very sensitive to mild uncoupling. *Biochem. Soc. Trans.* **31**, 1300-1301.
**Moses, K. and Rubin, G. M.** (1991). Glass encodes a site-specific DNA-binding protein that is regulated in response to positional signals in the developing Drosophila eye. *Genes Dev.* **5**, 583-593.
**Mourikis, P., Hurlbut, G. D. and Artavanis-Tsakonas, S.** (2006). Enigma, a mitochondrial protein affecting lifespan and oxidative stress response in Drosophila. *Proc. Natl. Acad. Sci. USA* **103**, 1307-1312.
**Mráček, T., Pecina, P., Vojtísková, A., Kalous, M., Sebesta, O. and Houstek, J.** (2006). Two components in pathogenic mechanism of mitochondrial ATPase deficiency: energy deprivation and ROS production. *Exp. Gerontol.* **41**, 683-687.
**Neretti, N., Wang, P. Y., Brodsky, A. S., Nyguyen, H. H., White, K. P., Rogina, B. and Helfand, S. L.** (2009). Long-lived Indy induces reduced mitochondrial reactive oxygen species production and oxidative damage. *Proc. Natl. Acad. Sci. USA* **106**, 2277-2282.
**Newmeyer, D. D. and Ferguson-Miller, S.** (2003). Mitochondria: releasing power for life and unleashing the machineries of death. *Cell* **112**, 481-490.
**Owusu-Ansah, E., Yavari, A., Mandal, S. and Banerjee, U.** (2008). Distinct mitochondrial retrograde signals control the G1-S cell cycle checkpoint. *Nat. Genet.* **40**, 356-361.
**Pan, D. A. and Hardie, D. G.** (2002). A homologue of AMP-activated protein kinase in Drosophila melanogaster is sensitive to AMP and is activated by ATP depletion. *Biochem. J.* **367**, 179-186.
**Pedersen, P. L., Ko, Y. H. and Hong, S.** (2000). ATP synthases in the year 2000: evolving views about the structures of these remarkable enzyme complexes. *J. Bioenerg. Biomembr.* **32**, 325-332.
**Robinson, K. M., Janes, M. S., Pehar, M., Monette, J. S., Ross, M. F., Hagen, T. M., Murphy, M. P. and Beckman, J. S.** (2006). Selective fluorescent imaging of superoxide in vivo using ethidium-based probes. *Proc. Natl. Acad. Sci. USA* **103**, 15038-15043.
**Ryoo, H. D., Domingos, P. M., Kang, M. J. and Steller, H.** (2007). Unfolded protein response in a Drosophila model for retinal degeneration. *EMBO J.* **26**, 242-252.
**Saleh, M. C., Fatehi-Hassanabad, Z., Wang, R., Nino-Fong, R., Wadowska, D. W., Wright, G. M., Harper, M. E. and Chan, C. B.** (2008). Mutated ATP synthase induces oxidative stress and impaired insulin secretion in beta-cells of female BHE/cdb rats. *Diabetes Metab. Res. Rev.* **24**, 392-403.
**Saxton, W. M., Porter, M. E., Cohn, S. A., Scholey, J. M., Raff, E. C. and McIntosh, J. R.** (1988). Drosophila kinesin: characterization of microtubule motility and ATPase. *Proc. Natl. Acad. Sci. USA* **85**, 1109-1113.
**Shevchenko, A., Wilm, M., Vorm, O. and Mann, M.** (1996). Mass spectrometric sequencing of proteins silver-stained polyacrylamide gels. *Anal. Chem.* **68**, 850-858.
**Smiley, S. T., Reers, M., Mottola-Hartshorn, C., Lin, M., Chen, A., Smith, T. W., Steele, G. D., Jr and Chen, L. B.** (1991). Intracellular heterogeneity in mitochondrial membrane potentials revealed by a J-aggregate-forming lipophilic cation JC-1. *Proc. Natl. Acad. Sci. USA* **88**, 3671-3675.
**Spradling, A. C. and Rubin, G. M.** (1982). Transposition of cloned P elements into Drosophila germ line chromosomes. *Science* **218**, 341-347.
**St Johnston, D.** (2002). The art and design of genetic screens: Drosophila melanogaster. *Nat. Rev. Genet.* **3**, 176-188.
**Sugiyama, S., Moritoh, S., Furukawa, Y., Mizuno, T., Lim, Y. M., Tsuda, L. and Nishida, Y.** (2007). Involvement of the mitochondrial protein translocator component tim50 in growth, cell proliferation and the modulation of respiration in Drosophila. *Genetics* **176**, 927-936.
**Talamillo, A., Chisholm, A. A., Garesse, R. and Jacobs, H. T.** (1998). Expression of the nuclear gene encoding mitochondrial ATP synthase subunit alpha in early development of Drosophila and sea urchin. *Mol. Biol. Rep.* **25**, 87-94.
**Towler, M. C. and Hardie, D. G.** (2007). AMP-activated protein kinase in metabolic control and insulin signaling. *Circ. Res.* **100**, 328-341.
**Viñas, O., Powell, S. J., Runswick, M. J., Iacobazzi, V. and Walker, J. E.** (1990). The epsilon-subunit of ATP synthase from bovine heart mitochondria. Complementary DNA sequence, expression in bovine tissues and evidence of homologous sequences in man and rat. *Biochem. J.* **265**, 321-326.
**Voos, W.** (2013). Chaperone-protease networks in mitochondrial protein homeostasis. *Biochim. Biophys. Acta*. **1833**, 388-399.
**Wilk, R., Pickup, A. T., Hamilton, J. K., Reed, B. H. and Lipshitz, H. D.** (2004). Dose-sensitive autosomal modifiers identify candidate genes for tissue autonomous and tissue nonautonomous regulation by the Drosophila nuclear zinc-finger protein, hindsight. *Genetics* **168**, 281-300.
**Wilkens, S.** (2000). F1F0-ATP synthase-stalking mind and imagination. *J. Bioenerg. Biomembr.* **32**, 333-339.
**Wingrove, J. A. and O'Farrell, P. H.** (1999). Nitric oxide contributes to behavioral, cellular, and developmental responses to low oxygen in Drosophila. *Cell* **98**, 105-114.
**Xie, M. and Roy, R.** (2012). Increased levels of hydrogen peroxide induce a HIF-1-dependent modification of lipid metabolism in AMPK compromised C. elegans dauer larvae. *Cell Metab*. **16**, 322-335.
**Xing, J., Liao, J. C. and Oster, G.** (2005). Making ATP. *Proc. Natl. Acad. Sci. USA* **102**, 16539-16546.
**Yates, J. R., III, Eng, J. K., McCormack, A. L. and Schieltz, D.** (1995). Method to correlate tandem mass spectra of modified peptides to amino acid sequences in the protein database. *Anal. Chem.* **67**, 1426-1436.